OXFORD

Original Article

Recombinant CC16 protein inhibits the production of pro-inflammatory cytokines via NF-κB and p38 MAPK pathways in LPS-activated RAW264.7 macrophages

Min Pang[1,†], Yangyang Yuan[2,†], Dong Wang[1], Ting Li[1], Dan Wang[1], Xiaohong Shi[3], Min Guo[4], Chunfang Wang[4], Xinri Zhang[1], Guoping Zheng[2,5], Baofeng Yu[2,*], and Hailong Wang[2,*]

[1]Department of Respiratory, The First Hospital, Shanxi Medical University, Taiyuan 030001, China, [2]School of Basic Medicine, Shanxi Medical University, Taiyuan 030001, China, [3]Department of Epidemiology, School of Public Health, Shanxi Medical University, Taiyuan 030001, China, [4]Center of Laboratory Animal, Shanxi Medical University, Taiyuan 030001, China, and [5]Centre for Transplantation and Renal Research, Westmead Millennium Institute, University of Sydney, Sydney NSW 2145, Australia

[†]These authors contributed equally to this work.

*Correspondence address. Tel/Fax: +86-351-4135772; E-mail: longwty@163.com (H.W.)/Tel/Fax: +86-351-4135670; Shanxiyangcheng@126.com (B.Y.)

Abstract

Accumulating evidence indicates that Clara cell protein-16 (CC16) has anti-inflammatory functions, although the involved molecular pathways have not been completely elucidated. Here, we evaluated the effect of recombinant rat CC16 (rCC16) on the expression of tumor necrosis factor alpha (TNF-α), interleukin-6 (IL-6), and IL-8 in lipopolysaccharide (LPS)-stimulated mouse macrophages (RAW264.7 cells) and explored the underlying molecular mechanisms. It was found that rCC16 inhibited LPS-induced TNF-α, IL-6, and IL-8 expression at both the messenger ribonucleicacid (mRNA) level and protein level in a concentration-dependent manner, as demonstrated by real-time reverse transcriptase-polymerase chain reaction and enzyme-linked immunosorbent assay. Such suppressive effects were accompanied by the inhibition of transcriptional activity and the deoxyribonucleic acid binding activity of nuclear factor (NF)-κB but not activator protein (AP)-1. Western blot analysis further revealed that rCC16 inhibited the increase of nuclear NF-κB and the reduction of cytosolic NF-κB, the phosphorylation and reduction of NF-κB inhibitory protein IκBα, and the p38 mitogen-activated protein kinase (MAPK)-dependent NF-κB activation by phosphorylation at Ser276 of its p65 subunit. Furthermore, rCC16 was found to have no effect on the phosphorylation of c-Jun N-terminal kinase, c-Jun, or the nuclear translocation of c-Jun. In addition, reduction of TNF-α, IL-6, and IL-8 were reversed when the level of endogenous uteroglobin-binding protein was reduced by RNA interference in rCC16- and LPS-treated RAW264.7 cells. Our data suggest that rCC16 suppresses LPS-mediated inflammatory mediator TNF-α, IL-6, and IL-8 production by inactivating NF-κB and p38 MAPK but not AP-1 in RAW264.7 cells.

Key words: recombinant rat CC16, pro-inflammatory cytokines, NF-κB, p38 MAPK, uteroglobin-binding protein

Introduction

Clara cell protein-16 (CC16) is mainly secreted by the non-ciliated, non-mucous-secreting club-shaped cells that are present throughout the respiratory tract [1]. Growing evidence shows that CC16 has anti-inflammatory activities in lung inflammation diseases, such as chronic obstructive pulmonary disease (COPD) and asthma [2,3], presumably via the inhibition of phospholipase A2 (PLA2) [4] and cytokine production [5]. Furthermore, studies of either human COPD cohorts or CC16-gene targeted mice in models of experimental COPD have indicated that reduced CC16 level contributes to the development and progression of COPD [6,7]. Thus, the administration of CC16 has been regarded as a novel disease-modifying therapy for COPD [2].

Pro-inflammatory cytokines play important roles in the development of COPD and asthma. Tumor necrosis factor alpha (TNF-α), interleukin-6 (IL-6), and IL-8 are produced by both inflammatory cells and primary lung epithelial cells in response to a variety of different stimuli [8,9]. TNF-α is a master cytokine during inflammation and a potent inducer of other pro-inflammatory chemokines and cytokines. It can induce the synthesis of eotaxin in lung epithelial cells; therefore, it plays a major role in coordinating mechanisms that command pro-inflammatory responses [10]. IL-6 is a multifunctional cytokine that is strongly involved in the regulation of inflammation, and both IL-6 and IL-8 [also named chemokine (C-X-C motif) ligand 8 (CXCL8)] are the major mediators and promoters for the recruitment and activation of neutrophils to regulate neutrophilic inflammation [11,12]. Based on the prominent roles of TNF-α, IL-6, and IL-8 in lung inflammatory disease, reducing the level of these cytokines is a strategy for treating inflammation.

In the present study, we pre-treated mouse macrophages (RAW264.7 cells) with recombinant rat CC16 protein (rCC16), followed by lipopolysaccharide (LPS) treatment. We demonstrated that rCC16 could suppress the messenger ribonucleic acid (mRNA) and protein levels of TNF-α, IL-6, and IL-8 via a nuclear factor (NF)-κB- and p38 mitogen-activated protein kinase (MAPK)-dependent mechanism rather than the activator protein (AP)-1. Moreover, we also found that rCC16 functioned as an anti-inflammation mediator through the 9-transmembrane protein uteroglobin-binding protein (UGBP). Our results suggest that the administration of rCC16 can reduce pro-inflammatory cytokines and relieve the inflammatory response.

Materials and Methods

Materials

RAW264.7 cell line was purchased from the Cell Culture Center of the Chinese Academy of Medical Sciences (Beijing, China). rCC16 protein was prepared according to published procedures [13]. Briefly, the open reading frame of rat CC16 gene was amplified and cloned into the pET-30a(+) vector (Novagen, Darmstadt, Germany). rCC16 expression was induced in *Escherichia coli* Rosetta(DE3) cells with 0.1 mM isopropy-β-D-thiogalactoside at 23°C and the rCC16 protein was purified by using Ni^{2+}-NTA agarose (Qiagen, Duesseldorf, Germany). The endotoxin contents in the protein preparations were removed and the concentration of endotoxin in the final purified proteins was <0.1 EU/ml. Purity of rCC16 was analyzed using 15% sodium dodecyl sulfate-polyacrylamide gel electrophoresis (SDS-PAGE) with Coomassie blue R250 staining and high-performance liquid chromatography (HPLC) system (Zorbax SB-C18; Agilant, Palo Alto, USA). The activity of rCC16 was assessed using PLA2 activity assay according to published procedures [13].

LPS was purchased from Sigma (St Louis, USA). Enzyme-linked immunosorbent assay (ELISA) kits specific for mouse TNF-α, IL-6, and IL-8 were purchased from Westang (Shanghai, China). Trizol reagent and an UltraSYBR Two-Step RT-qPCR Kit were purchased from CWBIO (Beijing, China). Dulbecco's modified Eagle's medium (DMEM)/high-glucose and fetal bovine serum (FBS) were obtained from Gibco (Grand Island, USA). The NE-PER Nuclear and Cytoplasmic Extraction Kit and bicinchoninic acid (BCA) protein assay reagent were purchased from Thermo Scientific (Waltham, USA). Cell Counting Kit-8 was purchased from Dojindo (Osaka, Japan). RIPA lysis buffer, protease/phosphatase inhibitor cocktail and X-tremeGENE HP deoxyribonucleic acid (DNA) Transfection Reagent were obtained from Roche (Mannheim, Germany).

Antibodies against NF-κB/p65, phosphorylated NF-κB/p65, p38, phosphorylated p38, c-Jun, phosphorylated c-Jun, c-Jun N-terminal kinases (JNK)1/2, phosphorylated JNK1/2, inhibitory factor IκBα, phosphorylated IκBα, β-actin, and lamin B were purchased from Cell Signaling Technology (Danvers, USA). Antibody against CC16 was purchased from Santa Cruz Biotechnology (Dallas, USA).

Cell culture and treatments

RAW264.7 cells were cultured in DMEM/high-glucose with 10% FBS in a humidified 5% CO_2 atmosphere at 37°C. Adherent cells were passaged every 3–4 days with a cell scraper. To determine the effect of rCC16 on cell viability, cells were cultured in 96-well plates at 1×10^4 cells/well and treated with 1.0, 2.5, or 5.0 μg/ml rCC16 for 1–5 days, and PBS of same volume was used as control. The culture medium was replaced by 100 μl of medium containing 10 μl of cell count kit-8 (CCK-8) per well, and incubated for another 3 h. Cell viability was measured using the Cell Counting Kit-8 according to the manufacturer's protocol. In addition, Trypan Blue exclusion assay was also used to assess the effect of rCC16 on cell viability. RAW264.7 cells were treated as above, and then harvested and stained with 0.4% Trypan Blue. The number of total and dead cells (stained) was counted using a hemocytometer. The percentage of viable cells is calculated as follows: Viable cells (%) = (Number of total cells − Number of dead cells)/Number of total cells × 100%

For the treatment of RAW264.7 cells, the serum-supplemented media were replaced by serum-free media. In the experiments including LPS treatments, subconfluent cultures of RAW264.7 cells were washed with PBS and then treated with 0.5, 1.0, or 2.0 μg/ml rCC16 for 2 h; then, 0.1 μg/ml LPS was added to the culture and incubated for another 0.5, 12, or 24 h. After treatment, culture supernatants or cells were harvested for analysis over three independent experiments.

For transfection experiments, RAW264.7 cells were seeded into 24-well plates at 1×10^5 cells/well and transfected with different plasmids using the X-tremeGENE HP DNA Transfection Reagent according to the manufacturers' protocols.

UGBP RNAi

The UGBP short hairpin ribonucleic acid (shRNA) plasmid was constructed according to the published research [14] using pRNAT-H1.1/hygro siRNA expression plasmid (GeneScript, Piscataway, USA). In the meantime, an expression plasmid encoding a non-relevant sequence shRNA (scrambled shRNA) was constructed as a control. The interference efficiency of shRNA plasmid targeting the endogenous UGBP was detected by transient transfection of UGBP shRNA construct into RAW264.7 cells, followed by real-time reverse transcriptase-polymerase chain reaction (RT-PCR). The targeted

mouse UGBP sequence is 5′-GCGAGTGCATCATCTCAAT-3′, the negative control sequence is 5′-TAAGGCTATGAAGAGATAC-3′.

Reverse transcriptase-polymerase chain reaction

After treatment with rCC16 and LPS or transfection with UGBP shRNA plasmid, RAW264.7 cells were harvested, and total ribonucleicacid (RNA) was extracted using the Trizol reagent. Real-time RT-PCR was performed on the Light Cycler® 480 PCR Instruments using the UltraSYBR Two-Step RT-qPCR Kit according to the manufacturer's instructions. Equal amounts of total RNA (1 μg) from each sample were converted into complementary DNA (cDNA) in a reverse-transcription reaction. PCR for each gene was carried out in a 20-μl reaction mixture containing 1 μl of cDNA template. The PCR conditions were 95°C for 1 min, followed by 40 cycles of 95°C for 10 s and 60°C for 40 s. The $2^{-\Delta\Delta CT}$ method was used to calculate the relative level of gene expression. The expression of the housekeeping gene *β-actin* was used as the internal control. The reactions were performed in triplicate for each sample. The primers were listed in **Table 1**.

To detect endogenous CC16 mRNA expression in RAW264.7 cells, total RNA was extracted using Trizol reagent, cDNA was synthesized, and CC16 was amplified according to the published protocols [15]. The mouse CC16 forward primer was 5′-ATGAAGATCGCCAT CACAATCA-3′, the reverse primer was 5′-GAATCTTAAATCTT GCTTACACAG-3′; and the *β-actin* was used as an internal control with the forward primer 5′-CACGATGGAGGGGCCGGACTCATC-3′ and the reverse primer 5′-TAAAGACCTCTATGCCAACACAGT-3′. The mouse lung cDNA library (provided by Prof. Rui Guo, Shanxi Medical University, Taiyuan, China) was used as a positive control.

Enzyme-linked immunosorbent assay

RAW264.7 cells were seeded in 12-well plates at 1×10^6 cells/well and cultured overnight. The cells were pre-treated with different concentrations of rCC16 for 2 h and then treated with 0.1 μg/ml LPS for another 24 h. The culture supernatants were collected to detect the TNF-α, IL-6, and IL-8 levels using the corresponding ELISA kit according to the manufacturer's instructions. To determine whether the UGBP is involved in the activities of rCC16, the UGBP shRNA plasmid and negative control plasmid were transfected into RAW264.7 cells. Twenty four hours later, the cells were pre-treated with 0 or 2.0 μg/ml rCC16 for 2 h and then treated with 0.1 μg/ml LPS for another 24 h. The levels of TNF-α, IL-6, and IL-8 in supernatants were measured by ELISA. All samples were examined in triplicate.

Luciferase reporter assay

RAW264.7 cells were seeded in 24-well plates at a density of 1×10^5 cells/well and were co-transfected with 0.5 μg of NF-κB or AP-1 promoter luciferase reporter plasmid and 0.02 μg of Renilla luciferase plasmid (Beyotime, Nantong, China) using X-tremeGENE HP DNA Transfection Reagent. After 24 h, 2.0 μg/ml rCC16 was added and incubated for 2 h, after which the cells were treated with 0.1 μg/ml LPS for another 24 h. The cells were lysed, and the Firefly luciferase activity was assayed and normalized to Renilla luciferase activity using a dual luciferase reporter assay system (Promega, Madison, USA).

Electrophoretic mobility shift assay

RAW264.7 cells were pre-treated with 2.0 μg/ml rCC16 for 2 h, followed by LPS treatment for another 1 h. Then, 5.0 μg of nuclear extract was incubated with 20 nM biotin-labeled double-stranded oligonucleotide probes (Beyotime, China) containing the consensus sequence for the NF-κB-DNA or AP-1-DNA-binding site for 20 min at room temperature and then separated on a non-denaturing 6% (w/v) polyacrylamide gel. The biotin-labeled oligonucleotide probes were transferred from the polyacrylamide gel onto a nylon membrane and then detected using the LightShift Chemiluminescent electrophoretic mobility shift assay (EMSA) kit (Thermo Scientific) according to the manufacturer's instructions.

Western blot analysis

Cold RIPA lysis buffer containing protease/phosphatase inhibitor cocktail and phenylmethanesulfonyl fluoride was used for total protein extraction. The NE-PER Nuclear and Cytoplasmic Extraction Kit was used for nuclear protein extraction. All of the proteins were quantified using the BCA protein assay reagent and then separated by 12% SDS-PAGE. Protein bands were electrophoretically transferred to a polyvinylidene fluoride membrane. The membrane was blocked with 5% skimmed milk, incubated overnight with the indicated antibodies at 4°C, and then incubated with HRP-conjugated anti-rabbit or anti-mouse immunoglobulin G for 1 h at room temperature. The protein bands were visualized using the electro-chemi-luminescence blot detection system (Pierce, Dallas, USA). To detect endogenous CC16 protein expression in RAW264.7 cells, the total protein extraction was prepared from RAW264.7 cells and the mouse lung total protein sample (provided by Prof. Rui Guo) was used as a positive control.

Statistical analysis

Data are presented as the mean ± SD. Student's *t*-test was used to compare two groups. Multiple-group comparisons were performed using S-N-K method after a one-way analysis of variance analysis. All of the statistical analyses were performed using the Statistical Package for the Social Sciences (SPSS) for Windows, version 13.0. Differences were considered statistically significant at P value < 0.05.

Results

rCC16 at low concentrations has no cytotoxic effect on RAW264.7 cells

SDS-PAGE with Coomassie blue R250 staining and HPLC assays showed that the purity of rCC16 was over 95%. rCC16 inhibited

Table 1. Primers used for quantitative real-time RT-PCR

Name	Forward primer (5′→3′)	Reverse primer (5′→3′)
TNF-α	TCCCAGGTTCTCTTCAAGGGA	GGTGAGGAGCACGTAGTCGG
IL-6	ACAAAGCCAGAGTCCTTCAGAG	GGTCCTTAGCCACTCCTTCTG
IL-8	CCGTCCCTGTGACACTCAAG	ACAGAAGCTTCATTGCCGGT
UGBP	TCAGTCCCAAAGTCTAAAGTCG	TTCCAAGATGTAACGCAACAG
β-actin	CTAAGGCCAACCGTGAAAAG	ACCAGAGGCATACAGGGACA

the activity of PLA2, which showed rCC16 had bioactivity [13]. First, we found that there was no endogenous CC16 expression in RAW264.7 cells as determined by RT-PCR and western blot assays (**Fig. 1A,B**). To investigate the cytotoxic effect of rCC16, RAW264.7 cells were treated with rCC16 at 1.0, 2.5, 5.0 μg/ml or PBS control, and the cell viability was assessed 1–5 days later. The effect of rCC16 on RAW264.7 cell proliferation and viability was assessed by CCK-8 assays and Trypan Blue staining, respectively. As shown in **Fig. 1C**, the treatment of RAW264.7 cells with rCC16 evoked a dose-dependent inhibition of cell proliferation compared to PBS controls, as determined by CCK-8 assays. The data showed that treatment of cells with 5 μg/ml rCC16 had an obvious cytotoxicity at Day 5. However, there was no difference in cell viability among treatments with different concentrations of rCC16 (**Fig. 1D**). These results suggest that the reduction of cell number observed at high concentrations of rCC16 is due to reduced cell proliferation rather than cell death. Taken together, our data indicate that rCC16 at low concentrations (2.5 μg/ml or lower) displays no cytotoxic effect on RAW264.7 cells.

rCC16 inhibits the expressions of TNF-α, IL-6, and IL-8 in LPS-stimulated RAW264.7 cells

RAW264.7 cells release various cytokines in response to stimulation with LPS [16]. To determine the potential effect of rCC16 on the production of pro-inflammatory cytokines, RAW264.7 cells were pre-treated with different dosages of rCC16 for 2 h, followed by stimulation with LPS (0.1 μg/ml) for 24 h. The mRNA and protein levels of the cytokines were measured by real-time PCR and ELISA assays, respectively. As shown in **Fig. 2**, LPS stimulation markedly increased the productions of TNF-α, IL-6, and IL-8, while the expressions of these LPS-stimulated cytokines were inhibited by rCC16 in a dose-dependent manner, being significant at concentrations over 1.0 μg/ml at the mRNA (**Fig. 2A–C**) and protein (**Fig. 2D–F**) levels. These results suggest that rCC16 effectively suppresses the production of pro-inflammatory cytokines in LPS-stimulated RAW264.7 cells.

rCC16 suppresses the transcriptional activity and DNA binding of NF-κB but not AP-1 in LPS-stimulated RAW264.7 cells

Because NF-κB and AP-1 have been implicated in the transcriptional activation of various inflammatory cytokines [17,18], the effects of rCC16 on these signaling pathways were investigated by luciferase reporter assay and EMSA. As shown in **Fig. 3A,B**, LPS caused an ~15- and 10-fold increase in the relative luciferase activity of NF-κB and AP-1, respectively, and rCC16 inhibited LPS-induced NF-κB transcriptional activity but had no effect on AP-1. To further verify the inhibitory effect of rCC16 on NF-κB but not AP-1 activity, EMSA was used to determine whether rCC16 could inhibit the DNA-binding activity of NF-κB or AP-1 using a biotin-labeled consensus p65 or c-Jun probe. As shown in **Fig. 3C,D**, LPS treatment augmented the p65 and c-Jun DNA-binding activities significantly, and rCC16 suppressed LPS-induced NF-κB-DNA binding but not AP-1-DNA binding. These findings indicate that rCC16 suppresses the transcriptional activity of NF-κB by blocking its DNA binding and that rCC16 has no effect on AP-1 activity.
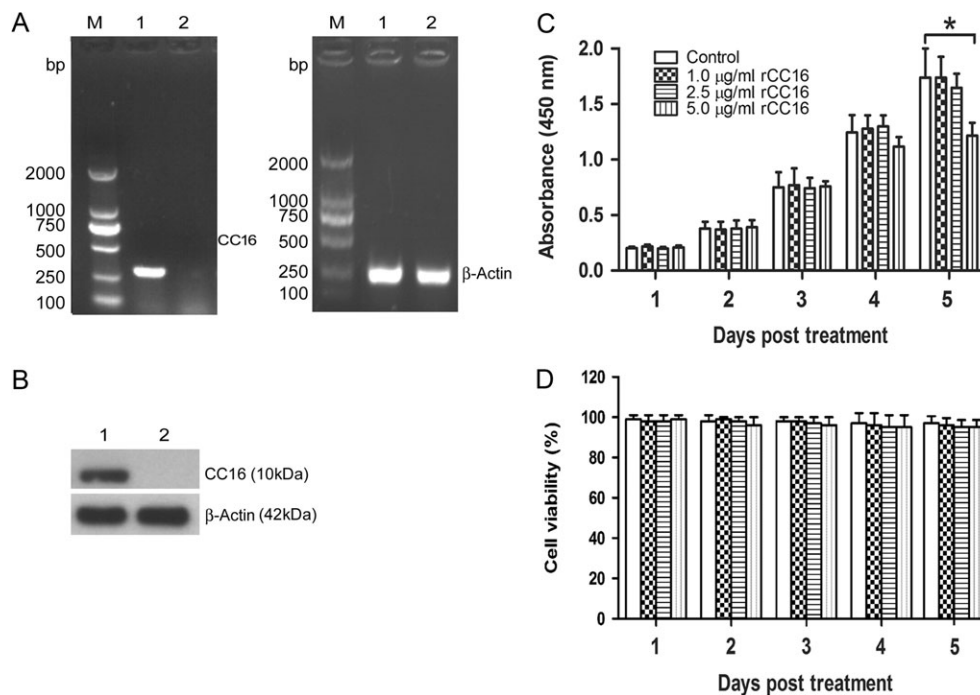

Figure 1. Endogenous expression of CC16 in RAW264.7 cells and effects of rCC16 protein on RAW264.7 cell viability (A,B) The endogenous CC16 expression in RAW264.7 cells was detected by RT-PCR (A) and western blot analysis (B). Lane M: DNA marker; Lane 1: positive control (mouse lung sample); Lane 2: RAW264.7 cells sample. β-Actin was used as an internal control. Each assay was repeated three times with similar results. (C,D) RAW264.7 cells were treated with 1.0, 2.5, or 5.0 μg/ml rCC16 or the same volume of PBS for 1–5 days, and cell proliferation and cell viability were determined by CCK-8 assays (C) and Trypan Blue staining (D), respectively. The data are presented as the mean ± SD of three independent experiments. *$P < 0.05$ relative to vesicle controls. RT-PCR, reverse transcriptase-polymerase chain reaction, DNA, deoxyribonucleic acid.
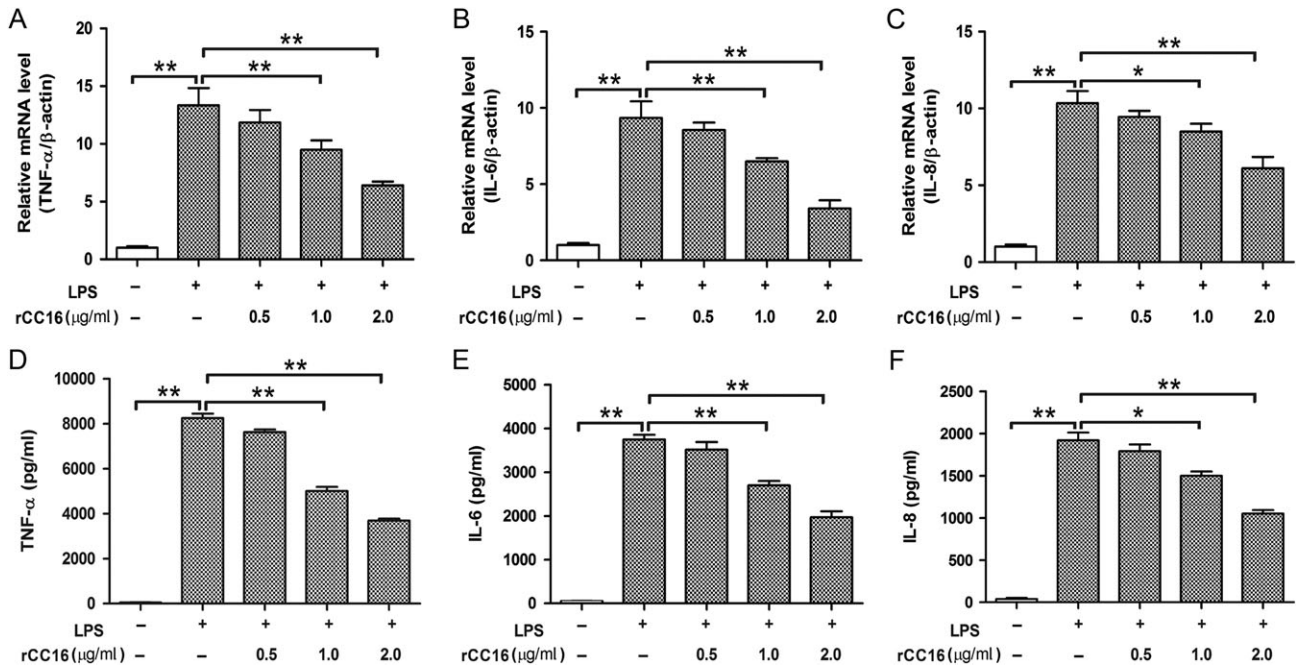
Figure 2. Effect of rCC16 on LPS-induced TNF-α, IL-6, and IL-8 expression in RAW264.7 cells (A–F) Real-time PCR (A–C) and ELISA assays (D–F) showed the inhibition of LPS-stimulated TNF-α, IL-6, and IL-8 expression by rCC16 in a concentration-dependent manner. RAW264.7 cells were incubated for 2 h with 0–2.0 μg/ml rCC16 and then exposed to 0.1 μg/ml LPS for another 24 h. For qPCR determinations, the results are expressed as ratios of $2^{-\Delta\Delta CT}$ qPCR values for TNF-α, IL-6, and IL-8 mRNA/β-actin. For ELISA determinations, the results are expressed as the absolute protein values of TNF-α, IL-6, and IL-8. The data are presented as the mean ± SD of three independent experiments. *$P < 0.05$ and **$P < 0.01$ indicate significant differences between groups as shown. qPCR, quantitative polymerase chain reaction; TNF-α, tumor necrosis factor alpha; IL-6, interleukin-6; LPS, lipopolysaccharide; mRNA, messenger RNA; ELISA, enzyme-linked immunosorbent assay.
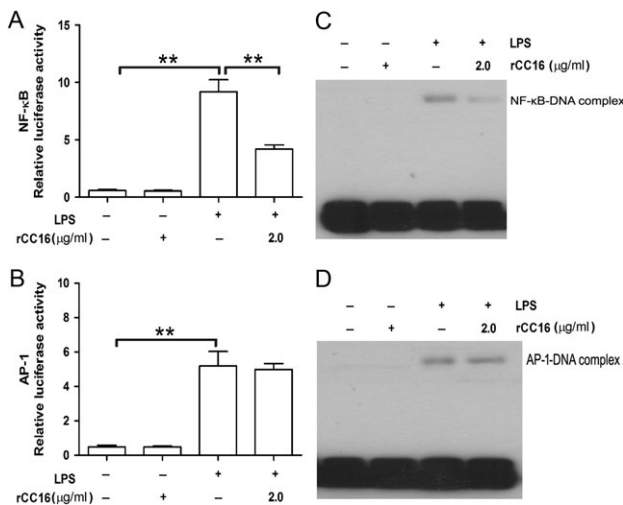

Figure 3. rCC16 inhibits the LPS-induced activation and DNA binding of NF-kB but not AP-1 transcription factors in RAW264.7 cells (A–D) Luciferase reporter assay (A, B) and EMSA (C, D) showed the suppression of the transcriptional activity (A) and DNA binding (C) of an NF-κB-responding promoter construct by rCC16 in RAW264.7 cells stimulated with 0.1 μg/ml LPS for 24 h (luciferase reporter assay) or 1 h (EMSA assay). rCC16 had no effect on AP-1 transcriptional activity (B) or DNA binding (D) under the same conditions. Each assay was repeated three times with similar results. The data are presented as the mean ± SD of three independent experiments. **$P < 0.01$ indicates significant differences between groups as shown. LPS, lipopolysaccharide; AP-1, activator protein; NF-κB, nuclear factor; DNA, deoxyribonucleic acid.

rCC16 attenuates LPS-induced NF-κB activation in RAW264.7 cells

NF-κB activation involves either the translocation of the p65 subunit into the nucleus or the phosphorylation of the p65 subunit. Thus, we investigated whether rCC16 inhibits p65 nuclear translocation and phosphorylation. As shown in **Fig. 4**A, an increased level of NF-κB/p65 in the nucleus was observed in LPS-treated cells, and this increase was significantly suppressed by rCC16. Consistently, a decreased level of cytosolic NF-κB/p65 was observed in LPS-treated cells, and rCC16 rescued this decrease under the same conditions. Western blot analysis also showed that LPS increased the phosphorylation of p65 at Ser276; the pretreatment of cells with rCC16 attenuated this phosphorylation without affecting the total level of p65 (**Fig. 4**B). These data suggest that the inhibition of NF-κB activity by rCC16 involves both the blockage of nuclear translocation and the phosphorylation of its p65 subunit in LPS-induced RAW264.7 cells.

rCC16 inhibits the LPS-induced phosphorylation of IκBα and p38 in RAW264.7 cells

The nuclear translocation and phosphorylation at Ser276 of the NF-κB/p65 subunit depend on the phosphorylation and degradation of its inhibitory unit IκB and p38 MAPK signaling pathway, respectively [19,20]. We, therefore, first tested whether the administration of rCC16 could result in the cellular phosphorylation and degradation of IκBα in LPS-stimulated RAW264.7 cells. As shown in **Fig. 5**A, LPS exposure resulted in the increased phosphorylation of IκBα, and the pretreatment of cells with rCC16 suppressed this phosphorylation. Meanwhile, the decrease in the cellular level of IκBα caused by LPS was attenuated by rCC16 pretreatment in a
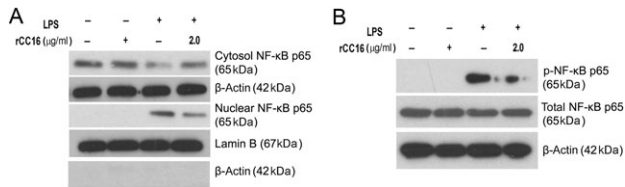
Figure 4. rCC16 prevents the nuclear translocation and phosphorylation of NF-κB/p65 in LPS-induced RAW264.7 cells RAW264.7 cells were treated with rCC16 at 2.0 μg/ml for 2 h and then exposed to LPS exposure at 0.1 μg/ml for another 1 h. (A,B) The subcellular distributions of NF-κB/p65 were determined by western blot analysis in the nuclear and cytoplasmic preparations (A), and the phosphorylation of NF-κB/p65 was detected by western blot analysis (B). The potential contamination of the nucleus-fractions by cytosol fractions was checked and excluded by western blot analysis using anti-β-actin antibody in the same samples. One representative of three independent experiments is shown. β-Actin and lamin B were used as cytosol-fraction or total cell extract and nucleus-fraction internal loading controls, respectively. LPS, lipopolysaccharide, NF-κB, nuclear factor.
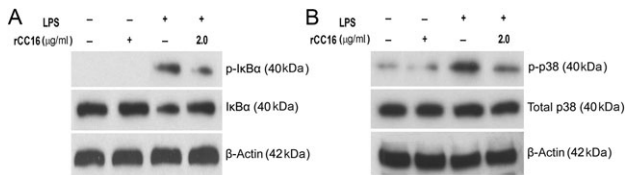

Figure 5. rCC16 inhibits the LPS-induced phosphorylation of IκBα and p38 MAPK in RAW264.7 cells RAW264.7 cells were treated with rCC16 at 2.0 μg/ml for 2 h and then exposed to LPS exposure at 0.1 μg/ml for another 1 h. The total proteins were extracted, and the levels of phosphorylated IκBα (A) and p38 MAPK (B) were detected by western blot analysis. The degradation of IκBα was detected by western blot analysis (A). One representative of three independent experiments is shown. β-Actin was used as an internal loading control. LPS, lipopolysaccharide.

similar pattern. Next, we investigated whether the decreased phosphorylation of the p65 subunit by rCC16 also involves p38 MAPK. As shown in **Fig. 5B**, rCC16 reduced the p-p38 level, but did not affect the total p38 level in LPS-stimulated RAW264.7 cells. These findings indicate that the rCC16 treatment of RAW264.7 cells prevents both the LPS-induced phosphorylation and degradation of IκBα. Moreover, rCC16 treatment also inhibits the activation of the p38 MAPK signaling pathway, which results in the phosphorylation at Ser276 of the NF-κB/p65 subunit in LPS-stimulated RAW264.7 cells.

rCC16 has no effect on the nuclear translocation of c-Jun or the phosphorylation of JNK and c-Jun in LPS-stimulated RAW264.7 cells

Accumulating evidence suggests that JNK and p38 MAPK are phosphorylated to activate the AP-1 transcription factor in LPS-treated macrophages [21,22]. We demonstrated that rCC16 had no effect on AP-1 activity in LPS-stimulated RAW264.7 cells, although it suppressed the phosphorylation of p38 under the same conditions (**Figs. 3C,D** and **5B**). These results inspired us to investigate the roles of rCC16 in the phosphorylation of JNK and c-Jun, the latter is the active subunit of AP-1 [23]. Western blot analysis results revealed that the phosphorylation of JNK and c-Jun was enhanced in LPS-treated RAW264.7 cells. Nevertheless, pretreatment with rCC16 did not alter this augment (**Fig. 6A**). Moreover, we examined the
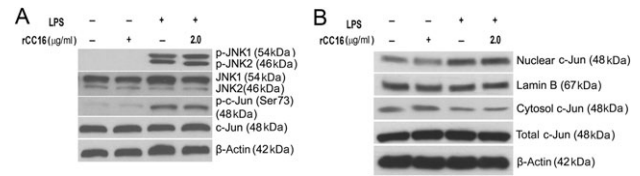

Figure 6. Effect of rCC16 on the nuclear translocation of c-Jun, phosphorylation of JNK and c-Jun in LPS-stimulated RAW264.7 cells RAW264.7 cells were treated with rCC16 at 2.0 μg/ml for 2 h and then exposed to LPS exposure at 0.1 μg/ml for another 1 h. (A) The total proteins were extracted, and the levels of phosphorylated JNK, c-Jun, and total JNK, c-Jun were detected by western blot analysis. (B) Subcellular distributions of c-Jun were determined by western blot analysis in nuclear and cytoplasmic preparations. One representative of three independent experiments is shown. β-Actin and lamin B were used as cytosol-fraction or total cell extract and nucleus-fractions internal loading controls, respectively. LPS, lipopolysaccharide; JNK, c-Jun N-terminal kinases .

nuclear translocation of c-Jun with or without rCC16 pretreatment in LPS-stimulated RAW264.7 cells. As shown in **Fig. 6B**, an augmented level of c-Jun in the nucleus was observed in LPS-treated cells, but this increase was not affected by rCC16. These findings imply that rCC16 treatment can not affect the nuclear translocation of c-Jun or the phosphorylation of JNK and c-Jun.

rCC16 exerts its anti-inflammatory effects via UGBP

It has been reported that UGBP acts as a receptor of CC16 and this protein is expressed in several cancer and normal cell types including RAW264.7 cells [24,25]. To test whether UGBP is involved in the inhibition of TNF-α, IL-6, and IL-8 by rCC16 in LPS-stimulated RAW264.7 cells, the endogenous UGBP was down-regulated by RNA interference and then the expression of pro-inflammatory cytokines was detected by ELISA. As shown in **Fig. 7**, quantitative RT-PCR result demonstrated that the endogenous UGBP in RAW264.7 cells was effectively suppressed (**Fig. 7A**). ELISA results showed that the production of TNF-α, IL-6, and IL-8 (**Fig. 7B–D**) was reversed in rCC16-pretreated and LPS-stimulated RAW264.7 cells when endogenous UGBP was down-regulated.

Discussion

COPD is a chronic lung disease characterized by unresolving inflammation due to the accumulation of activated neutrophils and T cells, causing small-airway obstruction. It has become a global epidemic due to increased air pollution and exposure to cigarette smoke. At present, bronchodilator and anti-inflammatory corticosteroids are widely used to treat all COPD patients; however, these approaches are disappointing because a certain number of COPD patients are resistant to corticosteroid treatment [26]. Therefore, alternative effective anti-inflammatory drugs are required.

CC16 with anti-inflammatory and immunomodulatory characteristics is mainly produced by the Clara cell which is present throughout the respiratory tract epithelium from the nose to the respiratory bronchioles [27]. Several human cohort and animal studies have shown that loss of CC16 airway expression contributes to the airway inflammation processes [28–30]. In our previous study, we demonstrated that rCC16 suppresses LPS-induced metalloproteinase (MMP)-9 expression in rat tracheal epithelial cells to reduce the inflammation response [13]. In the present study, we tested the effect of rCC16 on pro-inflammatory mediator production in
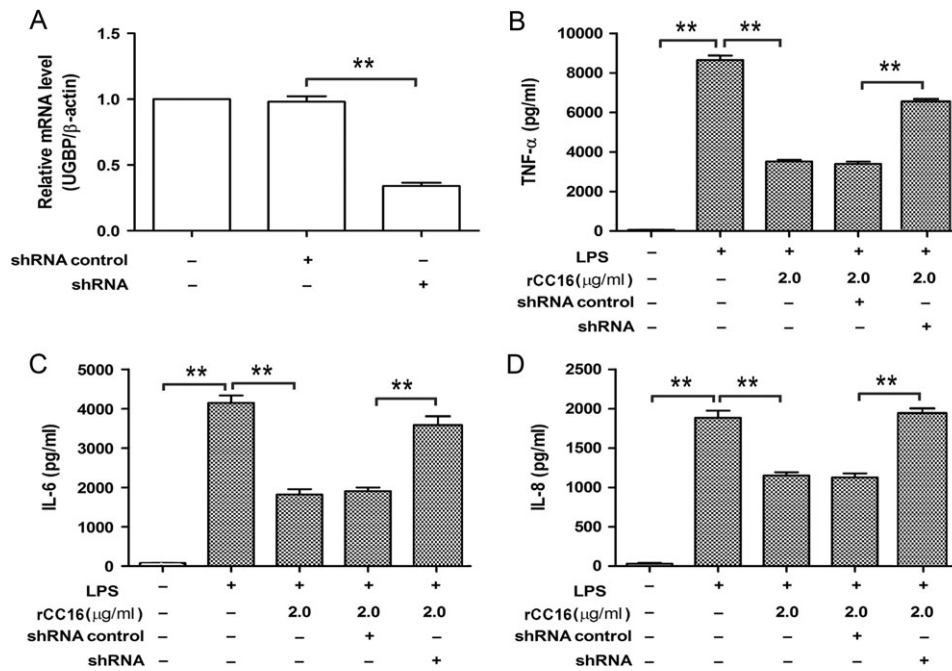
Figure 7. UGBP is involved in the anti-inflammatory role of rCC16 in LPS-stimulated RAW264.7 cells (A) RAW264.7 cells were transfected with UGBP shRNA plasmid or negative control plasmid. The mRNA levels of UGBP were detected by real-time RT-PCR. Each assay was repeated three times with similar results. (B–D) RAW264.7 cells were transfected with UGBP shRNA plasmid or negative control plasmid; after 24 h, cells were pre-treated with or without 2.0 μg/ml rCC16 for 2 h, and then exposed to 0.1 μg/ml LPS for another 24 h. The levels of TNF-α, IL-6, and IL-8 in supernatants were measured by ELISA. The data are presented as the mean ± SD of three independent experiments. **$P < 0.01$ indicate significant differences between groups as shown. TNF-α, tumor necrosis factor alpha; iL-6, interleukin-6; LPS, lipopolysaccharide; mRNA, messenger RNA; RT-PCR, reverse transcriptase-polymerase chain reaction. ELISA, Enzyme-linked immunosorbent assay; UGBP, uteroglobin-binding protein.

LPS-stimulated RAW264.7 cells to further demonstrate the anti-inflammatory activity of CC16.

We first analyzed the cytotoxic effect of rCC16 on RAW264.7 cells. Our data showed that rCC16 had no toxicity on cells when the concentration was <5.0 μg/ml. It has been shown that the over-expression of CC16 in immortalized bronchial epithelial cells delays the induction of anchorage independent growth [13,31]. Therefore, we used 2.0 μg/ml rCC16 or less in our present study.

Pro-inflammatory cytokines which are produced by both epithelial cells and immune cells, including macrophages and neutrophils, play an essential role in the development of air inflammation [32]. It has been reported that LPS binds to and activates toll-like receptor 4 [33] to induce signaling via conventional pro-inflammatory pathways, such as NF-κB, AP-1, and MAPK/extracellular signal-regulated kinase (ERK)/JNK/p38. Signaling through these pathways leads to an activation of the adaptive immune system and to the subsequent release of cytokines, such as TNF-α, IL-6, and IL-8 [17,22,34]. We therefore used LPS to determine its effect on TNF-α, IL-6, and IL-8 expression in RAW264.7 cells and the effectiveness of rCC16 as an anti-inflammation *in vitro*. Our data suggested that LPS indeed promoted TNF-α, IL-6, and IL-8 expression at both the mRNA and protein levels and that this effect was suppressed by rCC16 in a dose-dependent manner. We then examined the effect of rCC16 on LPS-induced NF-κB and AP-1 activation using reporter gene assays and EMSA analysis, since NF-κB and AP-1 are two of the key transcription factors, which are activated by LPS and have been implicated in regulating genes of the inflammatory cascade. We found that LPS could induce the transcriptional activation of NF-κB and AP-1. The transcriptional activity of NF-κB was suppressed together with the formation of NF-κB-DNA complexes by rCC16;

however, the activity of AP-1 was not affected by rCC16. These data showed that rCC16 inhibited the LPS-induced activation of NF-κB but not of AP-1.

We, therefore, investigated the effect of rCC16 on the nuclear translocation and phosphorylation of the NF-κB/p65 subunit, both of which are implicated in the activation of NF-κB [35–37]. Our results showed that rCC16 suppressed the nuclear translocation and phosphorylation of NF-κB/p65, which were increased by LPS. It is well known that the nuclear translocation of the NF-κB/p65 subunit depends on the phosphorylation and degradation of its inhibitor IκBα [35]. In addition, some evidence indicates that LPS can induce the phosphorylation of p38 MAPK [36] and then activate NF-κB via the phosphorylation of the p65 subunit at Ser276 [37]. Our results consistently showed that LPS promoted the phosphorylation and degradation of IκBα in LPS-treated RAW264.7 cells, and addition of rCC16 abolished this role of LPS. Meantime, we also found that rCC16 could reverse the phosphorylation of p38 without affecting its total level in LPS-stimulated RAW264.7 cells.

The AP-1 transcription factor is a dimeric complex composed of c-Jun/c-Jun or c-Jun/c-Fos. Usually, AP-1 activation is mainly induced by the phosphorylation and nuclear translocation of c-Jun [38,39]. The phosphorylation of Ser63 or Ser73 by JNK potentiates the ability of c-Jun to activate transcription [40]. In the present study, we found that the application of rCC16 did not inhibit the LPS-induced phosphorylation of JNK, phosphorylation of c-Jun or nuclear translocation of c-Jun. It has been reported that activated p38 could increase c-Fos expression and activate AP-1 activity to mediate inflammation [41]. Our results showed that rCC16 could attenuate the phosphorylation of p38 but not affect the AP-1 activity. Taken together, we propose that LPS triggered AP-1 activity

mainly through JNK/c-Jun other than the p38/c-Fos signaling pathway in our present study.

CC16, which is also called uteroglobin, is a glucocorticoid-inducible secretory protein [42]. It has been reported that uteroglobin can bind to UGBP which is a nine-transmembrane protein [43] and then induce the phosphorylation of ERK in NIH3T3 cells [14]. Moreover, UGBP has been shown to be expressed on RAW264.7 cells [24]. Therefore, we used RNA interference to down-regulate the UGBP expression and found that down-regulation of UGBP did affect the anti-inflammatory role of rCC16.

In conclusion, our results indicate that rCC16 decreases the production of the pro-inflammatory cytokines TNF-α, IL-6, and IL-8 in LPS-treated RAW264.7 macrophages by inactivating the NF-κB and p38 MAPK pathways rather than the AP-1 pathway. In addition, rCC16 exerts its anti-inflammatory effects via UGBP. These findings will allow us to gain further insight into the biological and molecular functions of CC16. Our observations indicate that CC16 augmentation approaches might have therapeutic efficacy in lung inflammatory disease.

References

1. Boers JE, Ambergen AW, Thunnissen FB. Number and proliferation of Clara cells in normal human airway epithelium. *Am J Respir Crit Care Med* 1999, 159: 1585–1591.

2. Laucho-Contreras ME, Polverino F, Tesfaigzi Y, Pilon A, Celli BR, Owen CA. Club cell protein 16 (CC16) augmentation: a potential disease-modifying approach for chronic obstructive pulmonary disease (COPD). *Expert Opin Ther Targets* 2016, 1–15.

3. Emmanouil P, Loukides S, Kostikas K, Papatheodorou G, Papaporfyriou A, Hillas G, Vamvakaris I, et al. Sputum and BAL Clara cell secretory protein and surfactant protein D levels in asthma. *Allergy* 2015, 70: 711–714.

4. Levin SW, Butler JD, Schumacher UK, Wightman PD, Mukherjee AB. Uteroglobin inhibits phospholipase A2 activity. *Life Sci* 1986, 38: 1813–1819.

5. Hung CH, Chen LC, Zhang Z, Chowdhury B, Lee WL, Plunkett B, Chen CH, et al. Regulation of TH2 responses by the pulmonary Clara cell secretory 10-kd protein. *J Allergy Clin Immunol* 2004, 114: 664–670.

6. Tsoumakidou M, Bouloukaki I, Thimaki K, Tzanakis N, Siafakas NM. Innate immunity proteins in chronic obstructive pulmonary disease and idiopathic pulmonary fibrosis. *Exp Lung Res* 2010, 36: 373–380.

7. Plopper CG, Mango GW, Hatch GE, Wong VJ, Toskala E, Reynolds SD, Tarkington BK, et al. Elevation of susceptibility to ozone-induced acute tracheobronchial injury in transgenic mice deficient in Clara cell secretory protein. *Toxicol Appl Pharmacol* 2006, 213: 74–85.

8. Marini M, Vittori E, Hollemborg J, Mattoli S. Expression of the potent inflammatory cytokines, granulocyte-macrophage-colony-stimulating factor and interleukin-6 and interleukin-8, in bronchial epithelial cells of patients with asthma. *J Allergy Clin Immunol* 1992, 89: 1001–1009.

9. Gerald CL, Romberger DJ, DeVasure JM, Khazanchi R, Nordgren TM, Heires AJ, Sisson JH, et al. Alcohol decreases organic dust-stimulated airway epithelial TNF-alpha through a nitric oxide and protein kinase-mediated inhibition of TACE. *Alcohol Clin Exp Res* 2016, 40: 273–283.

10. Sung HC, Liang CJ, Lee CW, Yen FL, Hsiao CY, Wang SH, Jiang-Shieh YF, et al. The protective effect of eupafolin against TNF-alpha-induced lung inflammation via the reduction of intercellular cell adhesion molecule-1 expression. *J Ethnopharmacol* 2015, 170: 136–147.

11. Taylor PR, Roy S, Leal SM Jr, Sun Y, Howell SJ, Cobb BA, Li X, et al. Activation of neutrophils by autocrine IL-17A-IL-17RC interactions during fungal infection is regulated by IL-6, IL-23, RORgammat and dectin-2. *Nat Immunol* 2014, 15: 143–151.

12. Gibson PG, Simpson JL, Saltos N. Heterogeneity of airway inflammation in persistent asthma: evidence of neutrophilic inflammation and increased sputum interleukin-8. *Chest* 2001, 119: 1329–1336.

13. Pang M, Wang H, Bai JZ, Cao D, Jiang Y, Zhang C, Liu Z, et al. Recombinant rat CC16 protein inhibits LPS-induced MMP-9 expression via NF-kappaB pathway in rat tracheal epithelial cells. *Exp Biol Med (Maywood)* 2015, 240: 1266–1278.

14. Li C, Wu Q. Adaptive evolution of multiple-variable exons and structural diversity of drug-metabolizing enzymes. *BMC Evol Biol* 2007, 7: 69.

15. Pang M, Yuan L, Zhang Z, Li D, Wang H. Construction of an eukaryocyte expression vector of mouse CCSP and identification of the activity of recombinant CCSP. *J Environ Health* 2015, 32: 899–902.

16. Li Y, Chi G, Shen B, Tian Y, Feng H. Isorhamnetin ameliorates LPS-induced inflammatory response through downregulation of NF-kappaB signaling. *Inflammation* 2016, 39: 1291–1301.

17. Anton L, Brown AG, Parry S, Elovitz MA. Lipopolysaccharide induces cytokine production and decreases extravillous trophoblast invasion through a mitogen-activated protein kinase-mediated pathway: possible mechanisms of first trimester placental dysfunction. *Hum Reprod* 2012, 27: 61–72.

18. Wu L, Li X, Wu H, Long W, Jiang X, Shen T, Qiang Q, et al. 5-Methoxyl aesculetin abrogates lipopolysaccharide-induced inflammation by suppressing MAPK and AP-1 pathways in RAW 264.7 Cells. *Int J Mol Sci* 2016, 17: 315.

19. Reber L, Vermeulen L, Haegeman G, Frossard N. Ser276 phosphorylation of NF-κB p65 by MSK1 controls SCF expression in inflammation. *PloS one* 2009, 4: e4393.

20. Kim HJ, Jeong JS, Kim SR, Park SY, Chae HJ, Lee YC. Inhibition of endoplasmic reticulum stress alleviates lipopolysaccharide-induced lung inflammation through modulation of NF-kappaB/HIF-1alpha signaling pathway. *Sci Rep* 2013, 3: 1142.

21. Park JG, Kim SC, Kim YH, Yang WS, Kim Y, Hong S, Kim KH, et al. Anti-inflammatory and antinociceptive activities of anthraquinone-2-carboxylic acid. *Mediators Inflamm* 2016, 2016: 1903849.

22. Nich C, Takakubo Y, Pajarinen J, Ainola M, Salem A, Sillat T, Rao AJ, et al. Macrophages-Key cells in the response to wear debris from joint replacements. *J Biomed Mater Res A* 2013, 101: 3033–3045.

23. Pan C, Xing JH, Zhang C, Zhang YM, Zhang LT, Wei SJ, Zhang MX, et al. Aldehyde dehydrogenase 2 inhibits inflammatory response and regulates atherosclerotic plaque. *Oncotarget* 2016, 7: 35562–35576.

24. Zhang TJ, Han JZ, Liu HJ, Liao XH, Li C, Luo ZQ. [Role of uteroglobin-binding protein in antiflammin-1 promoting IL-10 expression and secretion in RAW264.7 cells induced by endotoxin]. *Sheng Li Xue Bao* 2013, 65: 363–369.

25. Kundu GC, Mandal AK, Zhang Z, Mantile-Selvaggi G, Mukherjee AB. Uteroglobin (UG) suppresses extracellular matrix invasion by normal and cancer cells that express the high affinity UG-binding proteins. *J Biol Chem* 1998, 273: 22819–22824.

26. Jiang Z, Zhu L. Update on molecular mechanisms of corticosteroid resistance in chronic obstructive pulmonary disease. *Pulm Pharmacol Ther* 2016, 37: 1–8.

27. Irander K, Palm JP, Borres MP, Ghafouri B. Clara cell protein in nasal lavage fluid and nasal nitric oxide – biomarkers with anti-inflammatory properties in allergic rhinitis. *Clin Mol Allergy* 2012, 10: 4.

28. Park HY, Churg A, Wright JL, Li Y, Tam S, Man SF, Tashkin D, et al. Club cell protein 16 and disease progression in chronic obstructive pulmonary disease. *Am J Respir Crit Care Med* 2013, 188: 1413–1419.

29. Laucho-Contreras ME, Polverino F, Gupta K, Taylor KL, Kelly E, Pinto-Plata V, Divo M, et al. Protective role for club cell secretory protein-16

(CC16) in the development of COPD. *Eur Respir J* 2015, 45: 1544–1556.

30. Won TB, Quan SH, Rhee CS, Min YG, Lee CH. Expression of uteroglobin in a murine model of allergic rhinitis. *Acta Otolaryngol Suppl* 2007, 558: 83–89.

31. Linnoila RI, Szabo E, DeMayo F, Witschi H, Sabourin C, Malkinson A. The role of CC10 in pulmonary carcinogenesis: from a marker to tumor suppression. *Ann N Y Acad Sci* 2000, 923: 249–267.

32. Caramori G, Adcock IM, Di Stefano A, Chung KF. Cytokine inhibition in the treatment of COPD. *Int J Chron Obstruct Pulmon Dis* 2014, 9: 397–412.

33. Hoshino K, Takeuchi O, Kawai T, Sanjo H, Ogawa T, Takeda Y, Takeda K, *et al*. Cutting edge: Toll-like receptor 4 (TLR4)-deficient mice are hyporesponsive to lipopolysaccharide: evidence for TLR4 as the LPS gene product. *J Immunol* 1999, 162: 3749–3752.

34. Garcia MA, Gil J, Ventoso I, Guerra S, Domingo E, Rivas C, Esteban M. Impact of protein kinase PKR in cell biology: from antiviral to antiproliferative action. *Microbiol Mol Biol Rev* 2006, 70: 1032–1060.

35. Gilmore TD. Introduction to NF-kappaB: players, pathways, perspectives. *Oncogene* 2006, 25: 6680–6684.

36. Zhao D, Ding R, Mao Y, Wang L, Zhang Z, Ma X. Heparin rescues sepsis-associated acute lung injury and lethality through the suppression of inflammatory responses. *Inflammation* 2012, 35: 1825–1832.

37. Lee SJ, Shin JS, Choi HE, Lee KG, Cho YW, Ahn HJ, Jang DS, *et al*. Chloroform fraction of *Solanum tuberosum* L. cv Jayoung epidermis suppresses LPS-induced inflammatory responses in macrophages and DSS-induced colitis in mice. *Food Chem Toxicol* 2014, 63: 53–61.

38. Shaulian E, Karin M. AP-1 as a regulator of cell life and death. *Nat Cell Biol* 2002, 4: E131–E136.

39. Wang H, Song W, Hu T, Zhang N, Miao S, Zong S, Wang L. Fank1 interacts with Jab1 and regulates cell apoptosis via the AP-1 pathway. *Cell Mol Life Sci* 2011, 68: 2129–2139.

40. Li XM, Sun SZ, Wu FL, Shi T, Fan HJ, Li DZ. Study on JNK/AP-1 signaling pathway of airway mucus hypersecretion of severe pneumonia under RSV infection. *Eur Rev Med Pharmacol Sci* 2016, 20: 853–857.

41. Li JK, Nie L, Zhao YP, Zhang YQ, Wang X, Wang SS, Liu Y, *et al*. IL-17 mediates inflammatory reactions via p38/c-Fos and JNK/c-Jun activation in an AP-1-dependent manner in human nucleus pulposus cells. *J Transl Med* 2016, 14: 77.

42. Miele L, Cordella-Miele E, Facchiano A, Mukherjee AB. Novel anti-inflammatory peptides from the region of highest similarity between uteroglobin and lipocortin I. *Nature* 1988, 335: 726–730.

43. Kundu GC, Mantile G, Miele L, Cordella-Miele E, Mukherjee AB. Recombinant human uteroglobin suppresses cellular invasiveness via a novel class of high-affinity cell surface binding site. *Proc Natl Acad Sci USA* 1996, 93: 2915–2919.